J. metamorphic Geol., 2003, **21,** 761–769 doi:10.1046/j.1525-1314.2003.00477.x

On the mechanism of resorption zoning in metamorphic garnet

S. L. HWANG,[1] P. SHEN,[2] T. F. YUI,[3] AND H. T. CHU[4]
[1]*Institute of Materials Science and Engineering, National Dong Hwa University, Hualien, Taiwan*
[2]*Institute of Materials Science and Engineering, National Sun Yat-sen University, Kaohsiung, Taiwan (pshen@mail.nsysu.edu.tw)*
[3]*Institute of Earth Sciences, Academia Sinica, Taipei, Taiwan*
[4]*Central Geological Survey, PO Box 968, Taipei, Taiwan*

ABSTRACT An analytical electron microscope study of almandine garnet from a metamorphosed Al–Fe-rich rock revealed detailed composition profiles and defect microstructures of resorption zoning along fluid-infiltrated veins and even into the garnet/ilmenite (inclusion) interface. This indicates a limited volume diffusion for the cations in substitution (mainly Ca and Fe) and an interface-controlled partition for the extension of a composition-invariant margin. A corrugated interface between the Ca-rich margin/zone and the almandine garnet core is characterized by dislocation arrays and recovery texture further suggesting a resorption process facilitated by diffusion-induced recrystallization, diffusion-induced dislocation migration and diffusion–induced grain boundary migration. Integrated microstructural and chemical studies are essential for understanding the underlying mechanisms of processes such as garnet zoning and its modification. Without this understanding, it will not be possible to reliably use garnet compositions for thermobarometry and other applications that rely on garnet chemical information.

Key words: almandine garnet; analytical electron microscopy (AEM); diffusion mechanism; resorption zoning; retrograde metamorphism.

INTRODUCTION

The problem of retrograde zoning

Chemical zoning in igneous and metamorphic minerals, in particular growth zoning and diffusion zoning of garnet, has been extensively studied by electron probe microanalysis (EPMA). It is generally accepted that Fe, Mn and Mg homogenize in metamorphic garnet that has been heated to 650 °C or above for an extended period of time (Tracy, 1982). Compositional zoning of garnet cannot be used to decipher the 'closure' temperature or *P–T* paths (Spear *et al.*, 1984; Spear & Peacock, 1989; Frost & Tracy, 1991) if the rock of concern has a complex partition history, especially when solid-state diffusion or fluid infiltration has caused drastic garnet compositional changes during metamorphism. For example, when in contact with other phases from amphibolite facies rocks, garnet shows typically bell-shaped concentration profiles of Mn and/or Ca that can be attributed to growth zoning within garnet and limited cooling exchange reaction between the edges of coexisting phases (Tracy, 1982). On the other hand, Ca- and Mn-enrichment near grain rims due to limited lattice diffusion and effective intergranular element migration is characteristic of a resorption process during retrograde metamorphism (de Béthune & Laduron, 1975), although the underlying mechanism is not clear.

In this study, analytical electron microscopy (AEM) is used to characterize detailed composition and defect microstructures of resorption zoning of garnet. This zoning is presumably associated with fluid-infiltration veins, which are often filled with greenschist facies mineral assemblages that extend from the garnet margin to ilmenite inclusions in almandine garnet from metamorphosed Al–Fe-rich rocks. Local equilibrium during metamorphism is discussed and the solid-state diffusion mechanisms of resorption zoning, i.e. diffusion induced recrystallization (DIR) (Doo & Balluffi, 1958), diffusion induced grain boundary migration (DIGM) (Balluffi & Cahn, 1981), and diffusion induced dislocation migration (DIDM) (Chang & Loretto, 1988) known for a number of solid solution systems, are proposed.

SAMPLE DESCRIPTION

Location

Almandine garnet was found as a major mineral constituent in the Al–Fe-rich metamorphosed palaeo-weathering horizon of the Tananao Metamorphic complex in the Hoping area, eastern Taiwan (Yui *et al.*, 1994). The Al–Fe-rich rock with porphyroblastic garnet that has been characterized in detail is a thin (about 30–50 cm thick) layer in contact with marble on one side that changes gradually into metabasite on the other side. This particular Al–Fe-rich rock (denoted as HA-1) has very high contents of Al, Fe, Ti, K, Rb, Cs and Ba, which are believed to result from submarine weathering of a basaltic rock (Yui *et al.*, 1994).

Regional metamorphism

The Tananao Metamorphic Complex which consists of the western Tailuko belt and the eastern Yuli belt (Yen, 1963) forms the pre-Tertiary basement of Taiwan. It has experienced a complicated metamorphic and tectonic history. The Tailuko belt from which sample HA-1 comes has undergone subduction and high-pressure metamorphism during the mid-Jurassic; subduction and high-temperature metamorphism during the late Cretaceous; and subduction-collision accompanying high- to medium-pressure metamorphism during the late Cenozoic (Liou & Ernst, 1984; Yui *et al*., 1990, 1998). The mineral assemblage in HA-1 includes garnet, muscovite, chlorite, chloritoid, plagioclase, quartz, apatite and ilmenite. The rock has a porphyroblastic texture with *c*. 2 mm-size garnet porphyroblasts, with common micrometre-size inclusions of muscovite, chlorite, plagioclase, quartz, apatite and ilmenite. The estimated formation conditions of these matrix minerals are 5–7 kbar and 530–555 °C (Yui *et al*., 1992). Recent AEM observations (Hwang *et al*., 2001) further revealed submicron-size multiple-phase inclusions of kyanite, staurolite, quartz, zircon and brookite/rutile in almandine garnet. Peak metamorphic conditions of $>$ 8.3–8.8 kbar and $<$ 660–690 °C have been reported (Hwang *et al*., 2001). Fluids seem to have been important for the genesis of matrix minerals as evidenced by the pervasive decomposition of peak metamorphic minerals, such as kyanite and staurolite (Hwang *et al*., 2001, 2002). Rapid decompression could have produced the stress-related cracks in garnet, which allowed penetration of fluid into its margins.

Retrograde textures and analytical methods

The rock characterized in this study has been pervasively overprinted, so the original fabric is probably not preserved in the matrix. There are several sets of healed, semihealed and unhealed cracks in varied interspacings in garnet (Fig. 1a). The large cracks, filled with quartz and chlorite trend NW–SE (assuming N points towards the top of the micrograph) in the middle and north-eastern part of Fig. 1(a), appeared in a zigzag pattern with left-lateral stepping. (These fissure-filling minerals are consistent with the supposition that cracking and fluid infiltration took place in the retrograde stage, in particular under greenschist facies conditions.) It implies that the large cracks are crosscut by tiny sets of cracks that have more or less healed. The consistent orientation suggests that the large cracks were most probably related to unloading, as in the case demonstrated by Ji *et al*. (1997). Some of the tiny set of cracks likely emanated from micrometre-size inclusions of muscovite, chlorite, plagioclase, quartz, apatite and ilmenite as well as submicron-size multiple-phase inclusions of kyanite, staurolite, quartz, zircon and brookite/rutile as revealed by AEM (Hwang *et al*., 2001). They might be controlled by inclusion shape and size and require only modest decompression to initiate as indicated by the recent modelling of radial microcracks at the corners of inclusions in garnet using fracture mechanics (Whitney *et al*., 2000).

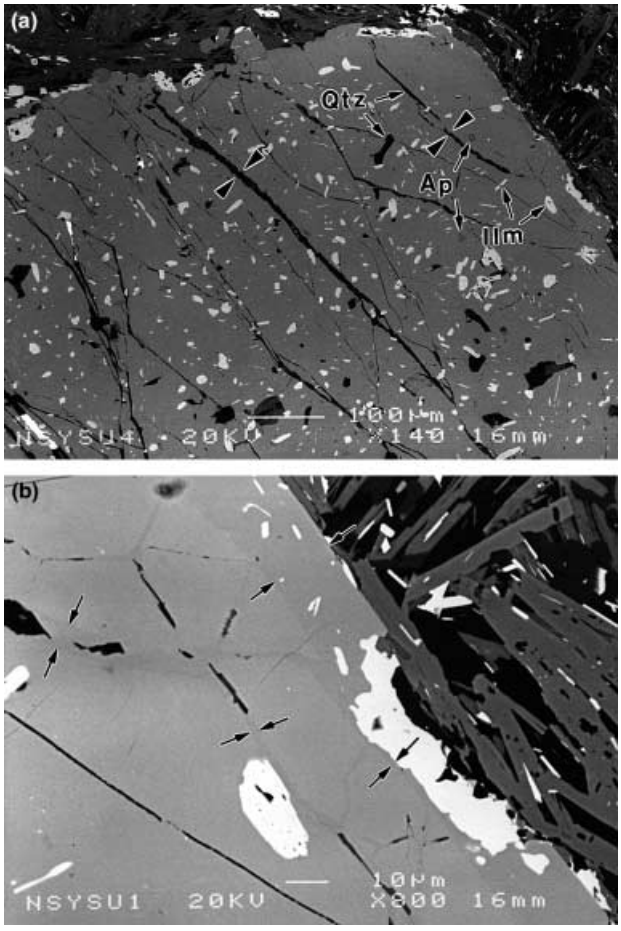

Fig. 1. SEM images (back-scattered electron image) of garnet from Al-Fe rich rock (HA-1) of the Tananao Metamorphic complex in the Hoping area, eastern Taiwan showing (a) ilmenite (Ilm) and apatite (Ap) inclusions and quartz (Qtz) filled cracks. Note the zigzag nature of quartz filled cracks as indicated by two opposite triangles. (b) Further magnified view from the right edge of (a) showing a Ca-rich zone about 30 μm wide which narrows down to 2–10 μm wide along the garnet/ilmenite interface or microcracks (grey zone between two opposite arrows), as indicated by darker contrast than garnet and EDX analysis.

Thin sections of sample HA-1 were studied by optical microscopy under plane polarized light. Two garnet crystals (LI-C-A & LI-C-B) were analyzed for resorption zoning and the results of sample LI-C-A were used as a typical example. Selected areas of garnet/ilmenite interface connected to open cracks and garnet rims were Ar-ion milled to electron transparency and then studied by transmission electron microscopy (TEM, JEOL 200CX at 200 kV) and analytical electron microscopy (AEM using JEOL instrument 3010 at 300 kV for imaging and composition analysis). Selected area electron diffraction (SAED) patterns were used to locate the garnet/ilmenite interface and the subgrain

boundaries of garnet for point count energy dispersive X-ray (EDX) analysis across the interface. Two beam (transmitted and diffracted beam, **g**) conditions, either in the bright field image or dark field image, were used to analyze the defect microstructures (mainly dislocations and their pile-ups) of the garnet associated with composition variations. The methods of defect analyses follow those used on spinel and pyrite (Hwang *et al.*, 1988). The polished surface of specimens were also studied by scanning electron microscopy (SEM, JSM6400 at 20 kV) to identify zones of the fluid infiltration along microcracks in garnet.

Bulk chemistry and zoning

SEM observations show that euhedral ilmenite and apatite grains clustered and coalesced next to and within the porphyroblastic garnet (Fig. 1a). A further magnified view (Fig. 1b) shows that the compositional zoning (in grey in Fig. 1b) is in association with the grain margins and microcracks/inclusions throughout the garnet. Typically, grey zones (between two opposite arrows in Fig. 1b) as wide as 30 μm can be identified by EDX analysis at garnet margins, but they narrow to *c*. 2–10 μm along either the garnet/ilmenite interface or open cracks (Fig. 1b). In all cases, the grey zones are characterized by chemical changes of originally almandine rich garnet, involving a decrease of almandine ($Fe_3Al_2Si_3O_{12}$) and pyrope ($Mg_3Al_2Si_3O_{12}$) components and an increase of the grossular ($Ca_3Al_2Si_3O_{12}$) component, analogous to the reported case of Ca- and Mn-rich rims in resorbed garnet (de Béthune & Laduron, 1975). The composition (in molar ratio) varied from 86.8% Alm, 6.2% Prp, 4.2% Grs, 2.6% Sps at garnet core to 76.3% Alm, 3.4% Prp, 17.9% Grs, 2.5% Sps at Ca-rich zones, based on AEM-EDX analysis, where Alm is almandine, Prp is pyrope, Grs is grossular, and Sps is spessartine.

AEM OBSERVATIONS

Distinct margin with fixed Ca content that is higher than garnet core

TEM montage images taken from one garnet/ilmenite interface near the garnet grain margin show a typical interface with characteristic dislocation array separating a 2–3 μm wide margin from the core (Fig. 2).

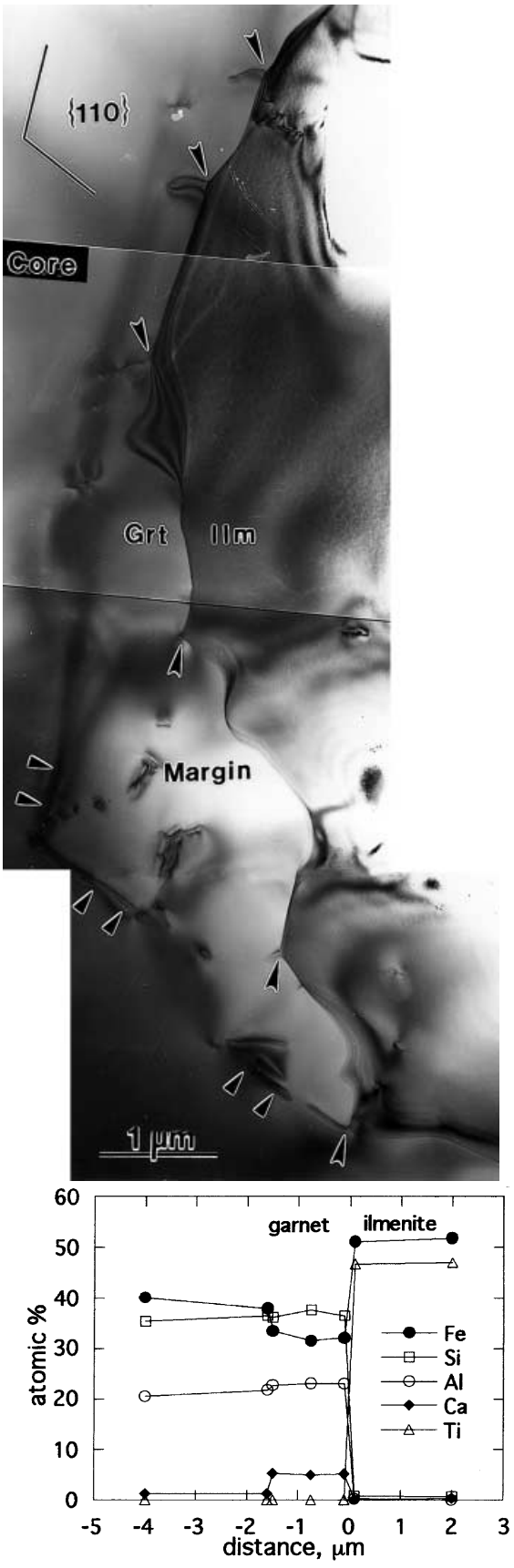

Fig. 2. TEM montage image (bright field images) of corrugated garnet/ilmenite (Grt/Ilm) interface near the garnet grain rim where a Ca-rich and Fe-poor zoning margin occurs as indicated by inset EDX profiles in orthogonal cross to the interface. Note the garnet margin is characterized by dislocations next to the garnet/ilmenite interface protrusions (arrows) on the garnet side, whereas the garnet core/margin interface by {110} facets (indicated by triangle pairs) parallel to the intersected crystallographic planes {110} denoted as solid lines.

Electron diffraction indicated that the margin has the same crystal structure and orientation as the garnet core. The concentration profiles based on the point count EDX analysis across the garnet/ilmenite interface further showed that the ilmenite is relatively invariant in composition, except at rims, in comparison with the chemical changes of garnet. Across the garnet margin, the Ca and Fe concentrations were found to be compensating, with relatively monotonous Si and Al values and traces of fluctuating Mg and Mn. Note that there is a nearly fixed content of grossular (*c.* 17–18 mol%) and almandine (*c.* 76–77 mol%) within the margin, implying a local equilibrium at core/margin interface via an interface controlled partition process as discussed later.

Zoning associated with (healed) microcracks and local chlorite

The Ca-rich and Fe-poor zoning was also found to be associated with fluid-infiltrated cracks of garnet, as shown by the composition profiles along the A-K trace in Figs 3 and 4. In this case, dislocations significantly climb to form faceted subgrain boundaries indicating a crystallographically controlled process as addressed later. Similar Ca-rich zoning was also found between garnet/ilmenite inclusion connected to the fluid-infiltrated cracks of garnet (Fig. 5a).

Ca-enrichment also defines a zone along healed microcracks (Fig. 6a) with local chlorite pockets (Fig. 6b). In this case, the relatively Ca-rich zoning is characterized by abundant dislocations delineating the original microcrack trace. Note that most dislocations in the zoning have been climbing from the crack surface into the garnet host, as indicated by the dislocation segments extending from the microcrack surface to the zoning boundaries. Depending upon the extent of almandine/grossular interdiffusion and the dislocation annihilation process discussed later, the dislocation may appear in a complex manner at healed cracks.

Irregular Ca-rich margin/zone of garnet against ilmenite

The garnet/ilmenite interface, located either near the garnet grain margin (Fig. 2) or connected to fluid-infiltrated open cracks within the garnet grains (Fig. 5a), is irregular and decorated with dislocations. The dislocations (indicated by arrows in Fig. 2) were frequently found to be attached to the protrusion parts of the corrugated garnet/ilmenite interface, suggesting that dislocation dragging is likely responsible for the wavy interface. By contrast, some euhedral ilmenite inclusions in garnet not connected to open cracks show an intact and characteristic flat garnet/ilmenite interface following the well developed (0001) surface of ilmenite (Fig. 5b). It should be noted that only garnet–ilmenite interface subjected to fluid-infiltration (resorption) shows wavy appearance. In this case, climbing dislocations accommodating the uneven interdiffusion of Ca and Fe could cause the interface to appear wavy. On the other hand, the flat/planar interface signifies that the intact area is immune from fluid infiltration.

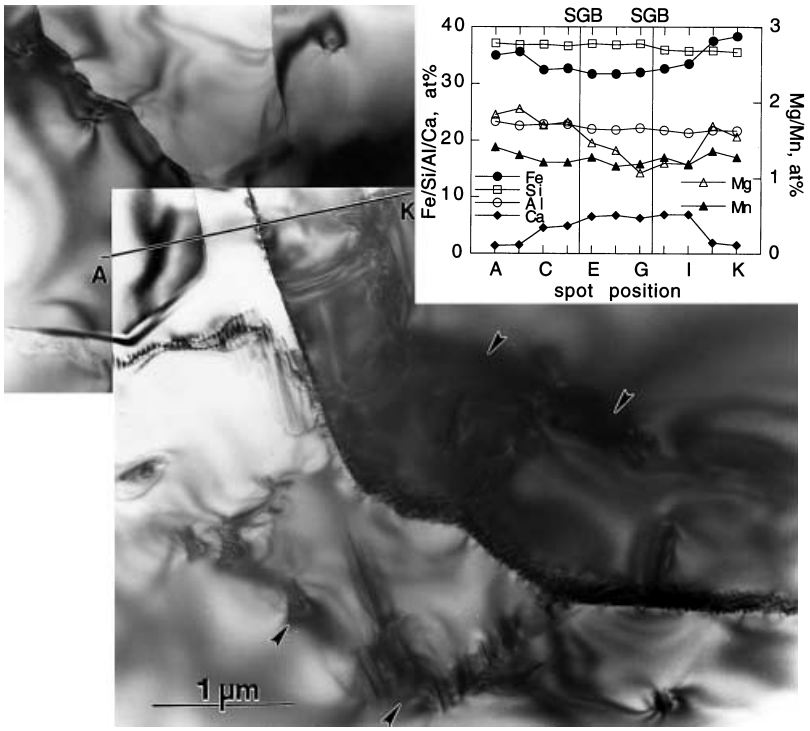

Fig. 3. TEM montage image (bright field images) and inset EDX profiles along A-K trace across two subgrain boundaries (SGB) of Ca-rich and Fe-poor zoning of garnet connected to a fluid-infiltrated crack, showing euhedral subgrains are bound by {110} surfaces and with different diffraction contrast across SGB. Note also climbing dislocations indicated by arrows.

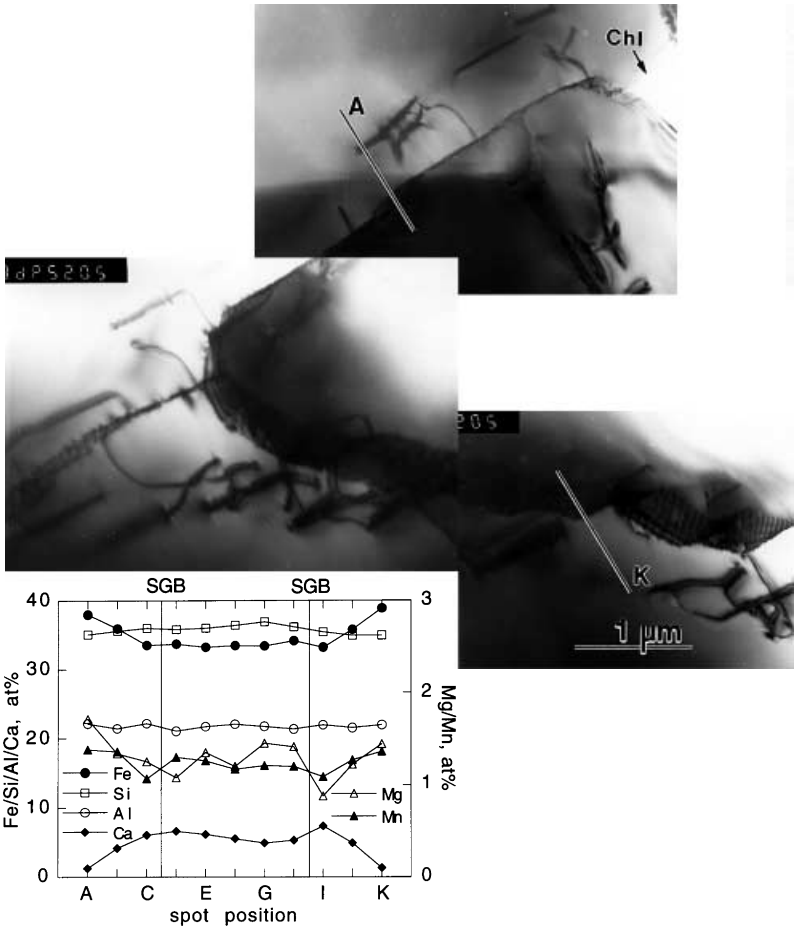

Fig. 4. TEM montage image (bright field images) and inset EDX profiles along A-K trace across two subgrain boundaries (SGB) of Ca-rich and Fe-poor zoning of garnet connected to a fluid-infiltrated crack filled with chlorite (Chl), showing a typical case of subgrain boundaries and climbing dislocations both being parallel to {110} of garnet.

Crystallographically controlled contact between garnet Ca-rich margin/zone and garnet core

Crystallographically controlled contacts between almandine garnet and Ca-rich zoning were observed near the garnet/ilmenite interface and also in the vicinity of open cracks filled with chlorite and quartz. In the former case, the contact between the garnet Ca-rich margin/zone and the garnet core runs approximately parallel to the {110} planes of garnet (Fig. 2). In the latter case, the garnet typically showed subgrains with rather straight boundaries and strong diffraction contrast due to strain effect (Figs 3 & 4). Strong dislocation contrast (arrows in Fig. 3) clearly delineate the boundaries of the Ca-rich regions. The subgrain core has the same composition as the intact garnet, whereas its 2–3 μm wide rim shows Ca-enrichment presumably a result of interdiffusion along the subgrain boundary (Fig. 3). A wider Ca-enrichment zoning toward the right of Fig. 4 can also be attributed to the process of subgrain boundary migration. Recovery process in such an area was manifest by the formation of low-energy {110} subgrain boundaries (Fig. 3) and dislocation arrays climbing away from the euhedral subgrain boundaries in a rather regular manner (Fig. 4). In general, the climbing dislocation arrays tend to have line segments parallel to {110}, the closed packed plane as well as the slip plane for garnet with a bcc-type Bravais lattice (Rabier & Garem, 1984; Karato, 1989). In this connection, it is noteworthy that the climb in grain boundary dislocations, as a result of the grain boundary Kirkendall effect, had once been proposed as one possible mechanism for the migration of high angle grain boundary upon interdiffusion of solute and solvent atoms with different diffusivities (Balluffi & Cahn, 1981). Subgrains of Ca-enrichment, which are bounded by {110} planes, are also frequently found along the garnet/ilmenite inclusion interface when connected to fluid-infiltrated and/or chloritization open cracks within the garnet grains (Fig. 7).

DISCUSSION

Cation substitution, dislocation generation and Ca source

Garnet retained the same crystal structure upon resorption zoning. This must be due to a wide composition tolerance for garnet structure with the following site specification. In fact, almandine garnet in

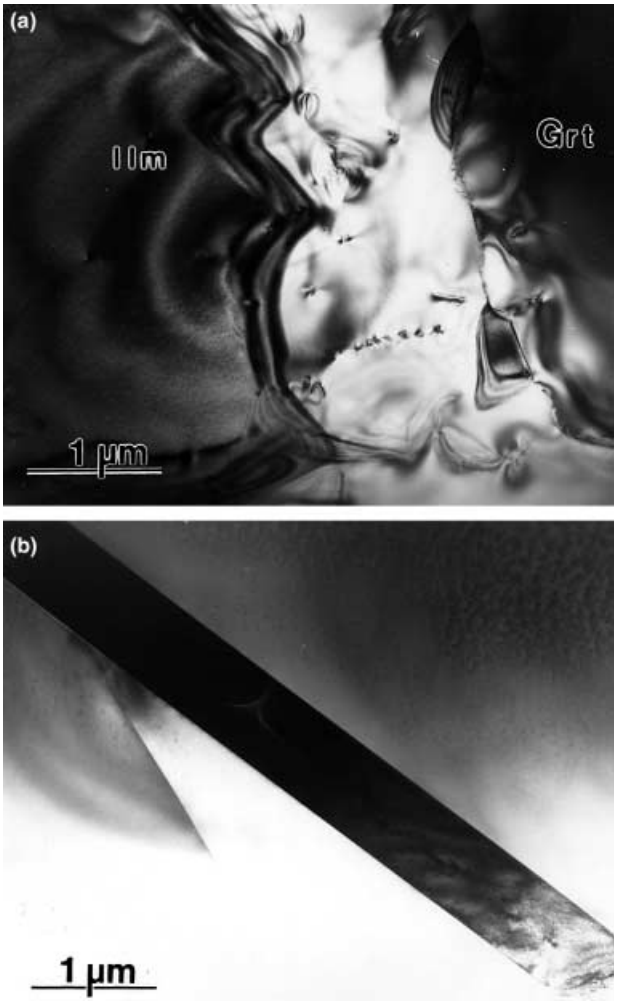

Fig. 5. TEM image (bright field image) of ilmenite inclusions (Ilm) in the interior of the garnet (Grt) crystal: (a) connected to fluid-infiltrated open cracks and a resultant Ca-rich garnet zoning along the Grt/Ilm interface. The zoning is characterized by corrugated Grt/Ilm and garnet core/margin interface and decorated with dislocations, giving different diffraction contrast for the garnet margin and core (b) intact ilmenite inclusion with well developed (0001) surface and imaged at Bragg condition.

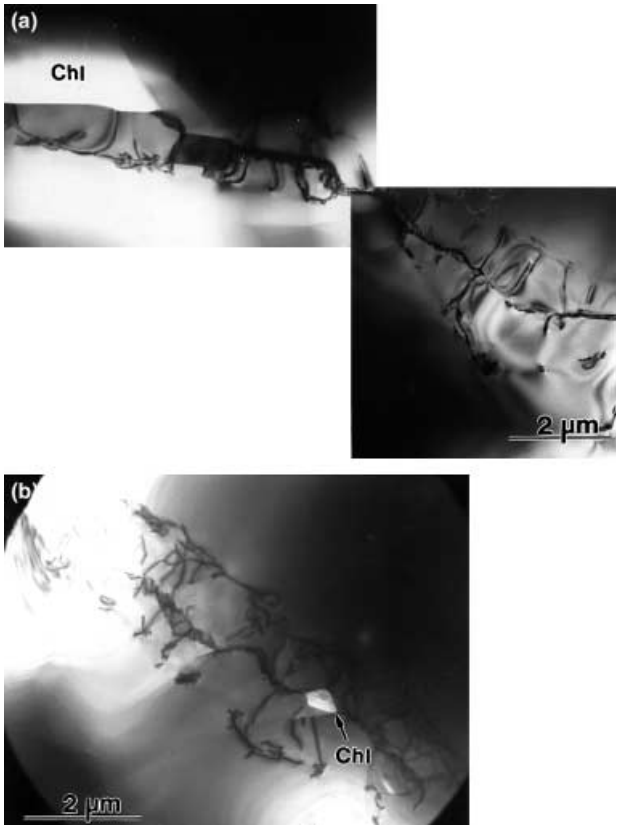

Fig. 6. TEM image (bright field images) of Ca-rich zoning along healed (110) cleavage: (a) extending from chlorite-filled microcrack (b) with relic chlorite pocket encompassed.

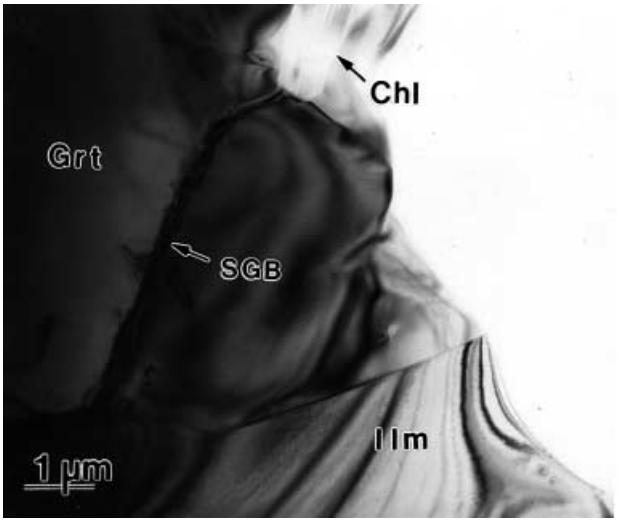

Fig. 7. TEM image (bright field image) of ilmenite inclusion (Ilm) in the interior of the garnet (Grt) crystal showing crystallographically controlled {110} SGB of garnet zoning connected to a fluid-infiltrated open crack filled with chlorite (Chl).

the space group of *Ia3d* contains eight $X_3Y_2Z_3O_{12}$ formula units in the unit cell, where X, Y and Z are divalent, trivalent and quadrivalent cations, respectively (Deer *et al.*, 1992). The structure consists of alternating ZO_4 tetrahedra and YO_6 octahedra which share corners to form a three-dimensional network. Within this network there are cavities that can be described as distorted cubes of eight oxygens containing the X ions (Novak & Gibbs, 1971).

Assuming a linear dependence in the composition of lattice parameters between the end members, the lattice parameters of the garnet matrix and the Ca-rich region are calculated as 1.1518 nm and 1.1596 nm, respectively. The lattice mismatch (ε) is then estimated to be (1.1596–1.1518)/1.1518 = 0.007, which is about an order of magnitude smaller than that required ($\varepsilon = 0.05$) for spontaneous loss of coherency (Brown & Woolhouse, 1970). However, the mismatch of Ca and

Fe in the individual dodecahedral site is much larger (22%) as indicated by the effective ionic radii of Ca^{2+} (0.112 nm) and Fe^{2+} (0.092 nm) in C.N. 8 (Shannon, 1976). The mismatch is even larger (+ 54%) if Ca^{2+} (0.100 nm) surprisingly enters octahedral site and thereby replaces Fe^{3+} (0.065 nm) with oxygen vacancies as charge compensating defects. Given such a high level of mismatch and distortion as a result of cation substitution in polyhedra sites, dislocations could be generated parallel to the {110} slip planes as observed to be the case (Fig. 4). Alternatively the dislocations could be from the garnet/ilmenite interface as indicated by a higher dislocation concentration at the protrusions of the wavy garnet/ilmenite interface. In any case, dislocations may climb as a result of unequal diffusivities of solute and solvent atoms across the core/margin interface.

Since the Ca enrichment is associated with garnet–ilmenite interface, along healed microcracks and chlorite–quartz veins, it may not be a result of garnet reaction with negligible plagioclase inclusions. Such a reaction during prograde metamorphism typically causes Ca-depletion rather than Ca-rich halos based on computer simulation (Frost & Tracy, 1991). During decompression for possible retrograde metamorphism, Ca content in garnet adjacent to plagioclase inclusions is either depleted (Whitney, 1991) or remains unchanged for high-grade metapelitic rocks (Lang, 1996), although retrograde diffusion within garnet may sometimes cause Ca-enrichment at the rim (e.g. Spear & Peacock, 1989). In the present case, it should be noted that intergranular rather than intracrystalline diffusion may prevail in retrograde metamorphism. Although plagioclase may not be directly involved, its presence in the matrix suggests that plagioclase (or other Ca-rich minerals, such as apatite) still may act as a Ca source through fluid infiltration during retrograde. The massive marble in direct contact with the Al–Fe-rich rock hosting the studied almandine garnet may be another possible Ca-source candidate. Alternatively, the Ca-rich zone garnet next to the local chlorite veins could be interpreted as a result of preferential diffusional loss of Fe and Mg (as well as Si and Al) if Ca has been conserved and the garnet volume has decreased adjacent to the veins. Obviously, this mechanism may be valid only when chlorite is nearby in the vein.

Partial and local equilibrium

Partial disequilibrium – meaning disequilibrium for some elements, but not for others – is known to be a common but rarely detected phenomenon during metamorphic mineral growth, even in ordinary prograde reactions subject to substantially different rates of intergranular diffusion coupled with intracrystalline diffusion (Carlson, 2002). It has been suggested that under lower greenschist facies conditions, Fe and Mg may equilibrate at hand-sample scale, whereas Mn and Ca may not equilibrate at millimetre-scale, because they may be subject to substantially different rates of intergranular diffusion (Carlson, 2002).

In the present case, Ca and Fe do not equilibrate at the millimetre-scale for garnet either. In fact, they have fixed values at the garnet margin next to the garnet/ilmenite interface or within subgrains next to the microcracks. Such a local equilibrium may appear to be fluid-assisted in view of previous observations of similar garnet composition along every surface that contains the mineral + fluid zone, irrespective of which mineral is in contact with garnet across the zone in amphibolite facies schists (Hames & Menard, 1993; Whitney *et al*., 1996).

Other explanations for retrograde zoning

Solid-state diffusion, either across or along an interphase interface or within a lattice, with dislocations, has been shown in a number of systems to introduce compositional and/or structural changes through the following mechanisms.

Diffusion-induced recrystallization

Diffusion induced recrystallization (DIR) can be triggered by volume-Kirkendall stresses in terms of unequal volume diffusion flows across diffusion couples (Doo & Balluffi, 1958) or along grain boundaries (den Broeder & Nakahara, 1983). We suggest that a DIR process during retrograde greenschist facies metamorphism should account for the newly formed subgrains or even grains at resorption zoning of almandine garnet. In other words, the garnet margin/zone was recrystallized during retrograde metamorphism. It is less likely that plastic deformation and the accompanying polygonization under the effect of applied stress (Poirier, 1985) occurred for garnet during the prograde amphibolite facies metamorphism (at 10–11 kbar and 500–630 °C: Hwang *et al*., 2001), because the garnet core did not show deformation induced dislocation arrays despite zoning that shows an increase in Fe content and a decrease in Mn from core to rim (Yui *et al*., 1992; Lu, 1992).

Diffusion–induced grain boundary migration

Diffusion induced grain boundary migration (DIGM), a grain boundary diffusion analogue of the Kirkendall effect, may proceed at relatively low temperatures (Balluffi & Cahn, 1981). In such a process, there is difference in atomic flux along the migrating grain boundaries. Since Ca^{2+} has the slowest diffusivity among the divalent cations (including Fe^{2+}) in garnet (Loomis, 1978; Loomis *et al*., 1985; Ganguly *et al*., 1998), the reverse zoning of garnet should have been controlled by the flux of Ca^{2+} in terms of DIGM in the episode of relatively low temperatures such as an overprinting greenschist facies metamorphism. It should be

noted that liquid film migration, a liquid-phase analogue of DIGM for the case of impurities causing the formation of a liquid phase at grain boundaries (Butler & Heuer, 1985) may not be excluded for fluid-assisted metasomatism of garnet rims during regional metamorphism (Hames & Menard, 1993; Whitney *et al.*, 1996). However beyond the far end of a microcrack, interface diffusion, rather than viscous flow in a continuous fluid of considerable thickness, must play an important role in corrugating the interface. In any case, the 'viscous' behaviour of grain boundaries has been verified experimentally for a number of metal polycrystals at high temperatures (Kê, 1947, 1949), suggesting that the intercrystalline slip occurs by thermal agitation within numerous 'disordered groups' of atoms at grain boundaries.

Diffusion-induced dislocation migration

Diffusion induced dislocation migration (DIDM), i.e. migration of dislocations to accommodate intracrystalline composition difference, was originally proposed to account for the rapidly solidified and then annealed polycrystals of metal alloy showing composition zones or core-shell structure with dislocation pile-ups at the core–shell interface (Chang & Loretto, 1988). The stress generated in the interface was suggested to help in the redistribution of these dislocations, and the driving force for the climb was provided by the excess energy of the supersaturated solid solution. Since there is a high level of mismatch where Ca^{2+} replaces Fe^{2+} in polyhedral sites to generate dislocations as mentioned, we suggest that a grain boundary diffusion analogue of such a DIDM process may be effective in the retrograde metamorphism which renders dislocations arrays in association with the resorption zoning front. In this regard, Kirkendall vacancies due to the unequal interdiffusion of Ca^{2+} and Fe^{2+} may facilitate the dislocation climb into arrays and thereby reduce the total strain energy. At relatively low temperatures, a dislocation annihilation process may still occur for garnet at the protrusions of the corrugated garnet/ilmenite interface and at a healing cleavage. In this connection, hot-stage SEM observations of $<110>$-type cracks in NaCl single crystal at 200 °C indicated that a dislocation annihilation process was the main cause for relaxation and healing of the deformed region near the crack (Park & O'Boyle, 1977). Finally it should be noted that diffusion along dislocations, i.e. pipe diffusion, is expected to be significant at relatively low temperatures (Porter & Easterling, 1981) to affect resorption zoning in metamorphic garnet.

CONCLUDING REMARKS

On the basis of defect microstructural observations of the garnet margins and garnet/inclusion interface associated with fluid infiltration, additional mechanisms of zoning in terms of grain boundary/pipe diffusion rather than simple volume diffusion are proposed in this article. The Ca/Fe composition profiles and dislocation arrays associated with chemical zoning of almandine garnet from a metamorphosed Al–Fe-rich rock indicated a resorption process involving DIR, DIGM and DIDM in terms of grain boundary and pipe diffusion beyond pervasive fluid-infiltrated veins. This defect-mediated resorption process with rather limited volume diffusion was associated with the overprinting retrograde greenschist facies metamorphism, whose P–T conditions are difficult, if not impossible to determine. Local equilibrium, i.e. solute partition at the zoning front in terms of short-circuit diffusion, is also characteristic of this resorption process. It is an open question whether the defect-mediated resorption zoning delineated here is valid only for specific exhumation processes. It would be also of great interest to explore the cases in which metamorphic reactions between garnet and inclusions/adjacent minerals, in particular anorthite-rich plagioclase, took place along P–T paths.

ACKNOWLEDGEMENTS

We thank Ms. L. C. Wang for her help with EDX analysis, Mr J. Chu for reading the manuscript, as well as Profs D. L. Whitney, B. R. Frost and an anonymous reviewer for constructive comments. This research is supported by National Science Council, Taiwan under contract NSC85-2111-M-214–001.

REFERENCES

Balluffi, R. W. & Cahn, J. W., 1981. Mechanism for diffusion–induced grain boundary migration. *Acta Metallurgica*, **29,** 493–500.

de Béthune, P. & Laduron, D., 1975. Diffusion processes in resorbed garnets. *Contributions to Mineralogy and Petrology*, **50,** 197–204.

den Broeder, F. J. A. & Nakahara, S., 1983. Diffusion induced grain boundary migration and recrystallization in the Cu-Ni system. *Scripta Metallurgica*, **17,** 399–404.

Brown, L. M. & Woolhouse, G. R., 1970. The loss of coherency of precipitates and the generation of dislocations. *Philosophical Magazine*, **21,** 329–345.

Butler, E. P. & Heuer, A. H., 1985. Grain boundary phase transformations during aging of a partially stabilized ZrO_2- a liquid-phase analogue of diffusion–induced grain boundary migration (DIGM) (?). *Journal of American Ceramic Society*, **68,** 197–202.

Carlson, W. D., 2002. Scales of disequilibrium and rates of equilibrium during metamorphism. *American Mineralogist*, **87,** 185–204.

Chang, C. P. & Loretto, M. H., 1988. Diffusion-induced dislocations in RSP Al-Mo. *Acta Metallurgica*, **36,** 805–810.

Deer, W. A., Howie, R. A. & Zussman, J., 1992. *An Introduction to the Rock-Forming Minerals*, 2nd edn. Longman Scientific and Technical, Essex.

Doo, V. Y. & Balluffi, R. W., 1958. Structural changes in single crystal copper-alpha brass diffusion couple. *Acta Metallurgica*, **6,** 428–438.

Frost, B. R. & Tracy, R. J., 1991. P-T paths from zoned garnets: some minimum criteria. *American Journal of Science*, **291,** 917–939.

Ganguly, J., Cheng, W. & Chakraborty, S., 1998. Cation diffusion in aluminosilicate garnets: experimental determination in pyrope-almandine diffusion couples. *Contributions to Mineralogy and Petrology*, **131,** 171–180.

Hames, W. E. & Menard, T., 1993. Fluid-assisted modification of garnet composition along rims, cracks, and mineral inclusion boundaries in samples of amphibolite facies schists. *American Mineralogist*, **78,** 338–344.

Hwang, S. L., Shen, P., Chu, H. T. & Jeng, R. C., 1988. Microstructures of chromium spinel and pyrite as indicators of thermomechanical history of Chromitite from Kenting melange, Taiwan. *Bulletin de Minéralogie*, **111,** 457–469.

Hwang, S. L., Yui, T. F., Chu, H. T. & Shen, P., 2001. Submicron polyphase inclusions in garnet from the Tananao Metamorphic Complex, Taiwan: a key to unraveling otherwise unrecognized metamorphic events. *Journal of Metamorphic Geology*, **19,** 599–605.

Hwang, S. L., Yui, T. F., Chu, H. T. & Shen, P., 2002. Discovery of kyanite/staurolite in the Tananao Metamorphic Complex, Taiwan: a (Suppl.). *Western Pacific Earth Sciences*, **2,** 161–170.

Ji, S., Zhao, P. & Saruwatari, K., 1997. Fracturing of garnet crystals in anisotropic metamorphic rocks during uplift. *Journal of Structural Geology*, **19,** 603–620.

Karato, S., 1989. Plasticity-crystal structure systematics in dense oxides and its implications for the creep strength of the earth's deep interior: a preliminary result. *Physics of the Earth and Planetary Interiors*, **55,** 234–240.

Kê, T. S., 1947. Experimental evidence of the viscous behavior of grain boundaries in metals. *Physical Review*, **71,** 533–546.

Kê, T. S., 1949. A grain boundary model and the mechanism of viscous intercrystalline slip. *Journal of Applied Physics*, **20,** 274–280.

Lang, H. M., 1996. Pressure-temperature-reaction history of metapelitic rocks from the Maryland Piedmont on the basis of correlated garnet zoning and plagioclase inclusion composition. *American Mineralogist*, **81,** 1460–1475.

Liou, J. G. & Ernst, W. G., 1984. Summary of Phanerozoic metamorphism in Taiwan. *Memoirs of the Geological Society of China*, **6,** 133–152.

Loomis, T. P., 1978. Multicomponent diffusion in garnet: II comparison of models with natural data. *American Journal of Science*, **278,** 1119–1137.

Loomis, T. P., Ganguly, J. & Elphick, S. C., 1985. Experimental determination of cation diffusivities in aluminosilicate garnets II. multicomponent simulation and tracer diffusion coefficients. *Contributions to Mineralogy and Petrology*, **90,** 45–51.

Lu, J. C., 1992. Metamorphic P-T-t path of the Hoping area, eastern Taiwan and its implications to the tectonic evolution. MSc Thesis, National Taiwan University, Taipei.

Novak, G. A. & Gibbs, G. V., 1971. The crystal chemistry of the silicate garnets. *American Mineralogist*, **56,** 791–825.

Park, S. M. & O'Boyle, D. R., 1977. Observations of crack healing in sodium chloride single crystals at low temperatures. *Journal of Materials Science*, **12,** L840–L841.

Poirier, J. P., 1985. *Creep of Crystals*. Cambridge University Press, Cambridge.

Porter, D. A. & Easterling, K. E., 1981. Phase Transformations in Metals and Alloys. *Van*. Nostrand Reinhold, New York.

Rabier, J. & Garem, H., 1984. Plastic deformation of oxides with garnet structure. In: *Materials Science Research*, Vol. 18 (eds Tressler, R. E. & Bradt, R. C.), pp. 187–198. Plenum Press, New York.

Shannon, R. D., 1976. Revised effective ionic radii in halides and chacogenides. *Acta Crystallographica*, **A32,** 751–767.

Spear, F. S. & Peacock, S. M., 1989. Metamorphic pressure-temperature-time paths. *Short Course in Geology*: 7. American Geophysical Union, Washington, DC.

Spear, F. S., Selverstone, J., Hickmott, D., Crowley, P. & Hodges, K. V., 1984. P-T paths from garnet zoning: a new technique for deciphering tectonic processes in crystalline terranes. *Geology*, **12,** 87–90.

Tracy, R. J., 1982. Compositional zoning and inclusions in metamorphic minerals. In: *Reviews in Mineralogy, 10. Characterization of metamorphism through mineral equilibria.* (ed. Ferry, J. M.), pp. 355–397. Mineralogical Society of America, Washington DC.

Whitney, D. L., 1991. Calcium depletion halos and Fe-Mn-Mg zoning around faceted plagioclase inclusions in garnet from a high-grade pelitic gneiss. *American Mineralogist*, **76,** 493–500.

Whitney, D. L., Cooke, M. L. & Du Frane, S. A., 2000. Modeling of radial microcracks at corners of inclusions in garnet using fracture mechanics. *Journal of Geophysical Research*, **105,** 2843–2853.

Whitney, D. L., Mechum, T. A., Dilek, Y. & Kuehner, S. M., 1996. Modification of garnet by fluid infiltration during regional metamorphism in garnet through sillimanite-zone rocks, Dutchess county, New York. *American Mineralogist*, **81,** 696–705.

Yen, T. P., 1963. The metamorphic belts within the Tananao schist terrain of Taiwan. *Proceedings of Geological Society of China*, **6,** 72–74.

Yui, T. F., Lan, C. Y., Heaman, L. & Chu, H. T., 1998. Late Cretaceous meta-andesite and late Jurassic (meta-) granite in the Tananao basement of Taiwan. *Abstract, Annual Meeting, Geological Society of China, Chungli, Taiwan*, 31.

Yui, T. F., Lu, C. Y. & Lo, C. H., 1990. Tectonic evolution of the Tananao Schist Complex of Taiwan. In: *Tectonics of Circum-Pacific Continental Margins* (eds Aubouin, J. & Bourgois, J.), pp. 193–209. VSP, The Netherlands.

Yui, T. F., Wang, Y., Wu, T. W., Lo, C. H., Lu, C. Y. & Chiao, C. H., 1992. Al-Fe-rich metamorphosed rock from the Tananao Metamorphic complex in the Hoping area, Taiwan: its metamorphic P-T path and origin. *Abstract, Annual Meeting, Geological Society of China, Tainan, Taiwan*, 68.

Yui, T. F., Wu, T. W., Wang, Y., Lo, C. H. & Lu, C. Y., 1994. Evidence for submarine weathering from metamorphosed weathering profiles on basaltic rocks, Tananao Metamorphic Complex, Taiwan. *Chemical Geology*, **118,** 185–202.

Received 4 December 2002; revision accepted 6 June 2003.